

See discussions, stats, and author profiles for this publication at: <https://www.researchgate.net/publication/230709623>

X-Ray Structure, Epr, and Magnetic-Susceptibility of Gallium(Iii) Tris(3,5-Di-Tert-Butyl-1,2-Semibenzoquinonate), a Main Group Triradical Complex

ARTICLE *in* INORGANIC CHEMISTRY · MARCH 1993

Impact Factor: 4.76 · DOI: 10.1021/ic00058a015

CITATIONS

41

READS

9

7 AUTHORS, INCLUDING:



Andrew Ozarowski

Florida State University

195 PUBLICATIONS 3,139 CITATIONS

SEE PROFILE



G. C. Defotis

College of William and Mary

84 PUBLICATIONS 446 CITATIONS

SEE PROFILE

X-ray Structure, EPR, and Magnetic Susceptibility of Gallium(III) Tris(3,5-di-*tert*-butyl-1,2-semibenzoquinonate), a Main Group Triradical Complex

Andrzej Ozarowski, Bruce R. McGarvey,* Ahmed El-Hadad, Zhigang Tian, and Dennis G. Tuck

Department of Chemistry and Biochemistry, University of Windsor, Windsor, Ontario N9B 3P4, Canada

Daniel J. Krovich and Gary C. DeFotis

Department of Chemistry, College of William and Mary, Williamsburg, Virginia 23185

Received August 28, 1992

The compound $\text{Ga}(\text{TBSQ}^\bullet)_3$ ($\text{TBSQ}^\bullet = 3,5\text{-di-}t\text{-butyl-1,2-benzosemiquinonate anion}$) has been prepared by two synthetic routes and its structure determined by X-ray analysis. The crystals are rhombohedral, with $a = 16.408(6)$ Å, $c = 13.898(4)$ Å, $V = 3240(2)$ Å³, $Z = 3$, and space group $R\bar{3}(h)$; $R = 0.050$; $T = 23$ °C. The molecule has a distorted octahedral GaO_6 kernel, with bidentate TBSQ^\bullet ligands. The compound and its solutions in noncoordinating solvents are stable for months, even when exposed to air. Frozen solution EPR spectra display evidence for the thermal occupation of both quartet, $S = 3/2$, and doublet, $S = 1/2$, states. A triradical should have both states, and comparison of theoretical simulations of the triradical EPR spectrum with the experimental spectrum reveals that the energy separation of the quartet and two doublet states is greater than 0.8 cm^{-1} and less than 20 cm^{-1} . $\text{Ga}(\text{TBSQ}^\bullet)_3$ reacts with pyridine to give $\text{Ga}(\text{TBSQ}^\bullet)(\text{TBC})(\text{py})_2$ ($\text{TBC} = 3,5\text{-di-}t\text{-butylcatecholate dianion}$). Magnetic susceptibility was measured for solid $\text{Ga}(\text{TBSQ}^\bullet)_3$ from 2 to 296 K and for the toluene solution at 296 K. The low-temperature susceptibilities show that the ground state is the doublet states of the triradical, and the high-temperature susceptibilities can only be explained by postulating another thermally accessible doublet state, which is close in energy to the triradical states. This state is postulated to be $\text{Ga}(\text{TBSQ}^\bullet)(\text{TBC})(\text{TBQ})$ ($\text{TBQ} = 3,5\text{-di-}t\text{-butyl-1,2-benzoquinone}$).

Introduction

In recent papers from this department, we have discussed the reactions between various main group metals and substituted *o*-benzoquinones. With magnesium, zinc, cadmium or barium, reaction with 3,5-di-*tert*-butyl-1,2-benzoquinone (TBQ) in refluxing toluene gave the diradical species $\text{M}(\text{TBSQ}^\bullet)_2$ ($\text{TBSQ}^\bullet = 3,5\text{-di-}t\text{-butyl-1,2-benzosemiquinonate anion}$)¹ while the analogous reaction with indium yielded the unusual indium(I) species $\text{In}(\text{TBSQ})$, whose oxidative and complexing reactions were investigated.² Corresponding experiments with the tetrahalogeno-*o*-quinones $\text{X}_4\text{C}_6\text{O}_2\text{-}o$ ($\text{X} = \text{Cl}, \text{Br}$) and either gallium or indium gave derivatives of the M^{II} state, stabilized as adducts such as $[\text{M}(\text{O}_2\text{C}_6\text{X}_4)\text{phen}]_2$ ($\text{phen} = 1,10\text{-phenanthroline}$).³ It therefore seemed logical to investigate the gallium/TBQ system, and we now report the direct synthesis of the gallium(III) complex $\text{Ga}(\text{TBSQ}^\bullet)_3$, which can also be prepared by an alternative route using GaI_3 and $\text{Na}^+\text{TBSQ}^\bullet$. The magnetic properties, EPR spectra, and the molecular structure have also been completely characterized.

The preparation of $\text{M}(\text{DTBSQ})_3$ triradical compounds ($\text{DTBSQ}^\bullet = 3,6\text{-di-}t\text{-butyl-1,2-benzosemiquinonate anion}$) ($\text{M} = \text{Al}, \text{Ga}$ or In) has been reported,⁴ but no isolation or analysis of the compounds was done, and the identification was based entirely upon the observation of an $S = 3/2$ EPR spectrum in frozen solution. This spectrum was identified by the presence of both $\Delta M = 2$ and $\Delta M = 3$ transitions, but no other analysis of the spin-Hamiltonian was reported. A triradical system should have two EPR active $S = 1/2$ states, in addition to the $S = 3/2$ state,

but no evidence of these transitions, or of transitions between the quartet and doublet states, were noted. Using the theory of triradicals developed below, the $S = 3/2$ spectra reported indicate that the energy separation between the quartet and doublet states must be greater than 0.3 cm^{-1} . This large energy separation of the spin states is surprising, considering that for the $\text{M}(\text{TBSQ}^\bullet)_2$ biradicals studied earlier we found that the energy separation between the $S = 1$ and $S = 0$ states (exchange energy) was very small.¹ The evidence for this was the observation in liquid solution of an EPR spectrum identical to that of the $S = 1/2$ spectrum of TBSQ^\bullet radicals with a doublet hyperfine splitting from one proton, because any exchange interaction greater than the hyperfine interaction parameter would produce a spectrum with a triplet hyperfine pattern from the two equivalent protons on the two semiquinone rings of the biradical. No hyperfine splittings from protons were reported for the $\text{M}(\text{DTBSQ}^\bullet)_3$ triradicals.⁴

Experimental Section

General Data. Gallium metal, 3,5-di-*tert*-butyl-1,2-benzoquinone (Aldrich) and sodium hydride (Aldrich) were used as supplied. Toluene was dried over sodium hydride and distilled before use. All preparative work was carried out in an atmosphere of dry nitrogen.

Gallium analysis was by atomic absorption spectrophotometry, using an IL-251 instrument; microanalysis was by Canadian Microanalytical Services Ltd. Infrared spectra in the $200\text{--}4000\text{-cm}^{-1}$ region were recorded on a Nicolet 5DX instrument, using KBr disks.

Preparation of $\text{Ga}(\text{TBSQ}^\bullet)_3$. (i) Gallium metal (0.20 g, 2.87 mmol) and TBQ (1.90 g, 8.61 mmol) were refluxed together in toluene; the wine-red color of the initial solution discharged during the first hour, and after a period of 24 h, a dark green solution was obtained. No gallium metal was recovered after filtering the cooled mixture. Removal of solvent gave green crystals (2.05 g, 98% yield). Anal. Calcd for $\text{C}_{42}\text{H}_{60}\text{O}_6\text{Ga}$: Ga, 9.54; C, 69.0; H, 8.28. Found: Ga, 10.0; C, 69.0; H, 7.91. The infrared spectrum showed that $\nu(\text{C}=\text{O})$ of TBQ, observed at 1654 cm^{-1} , was absent in the product; $\nu(\text{C}-\text{O})$ modes were observed at 1575, 1532 and 1487 cm^{-1} .

(ii) Gallium(III) iodide was prepared by refluxing the metal and iodine in toluene, followed by crystallization. Subsequently, 3,5-di-*tert*-

* Author to whom correspondence should be addressed.

- (1) Ozarowski, A.; McGarvey, B. R.; Peppe, C.; Tuck, D. G. *J. Am. Chem. Soc.* **1991**, *113*, 3288.
- (2) Annan, T. A.; McConville, D. H.; McGarvey, B. R.; Ozarowski, A.; Tuck, D. G. *Inorg. Chem.* **1989**, *28*, 1644.
- (3) Annan, T. A.; Tuck, D. G. *Can. J. Chem.* **1989**, *67*, 1807.
- (4) Prokof'ev, A. I.; Bubnov, N. N.; Solodovnikov, S. P.; Kabachnik, M. I. *Dokl. Chem. (Engl. Transl.)* **1979**, *245*, 178.

Table I. Summary of Crystal Data Intensity Collection and Structure Refinement for $\text{Ga}(\text{TBSQ}^*)_3$

chem formula	$\text{GaC}_{42}\text{H}_{60}\text{O}_6$
fw	730.65
cell consts, Å	$a = 16.408(6)$ $c = 13.898(4)$
cell vol, Å ³	3240(2)
space group	$R3(h)$ (No. 146)
Z ; $F(000)$	3; 1173
D_{calc} , g/cm ³	1.123
temp, °C	23
total no. of refls measd	1412
no. of unique data used	528 ($I \geq 3\sigma(I)$)
$R(F_o^2)^a$	0.050
$R_w(F_o^2)^b$	0.049
$\Delta\rho_{\text{max}}$, e Å ⁻³	0.24
max shift/error in final cycle	0.02

$$^a R = \sum ||F_o| - |F_c|| / \sum |F_o|. \quad ^b R_w = [\sum w(|F_o| - |F_c|)^2 / \sum w|F_o|^2]^{1/2}.$$

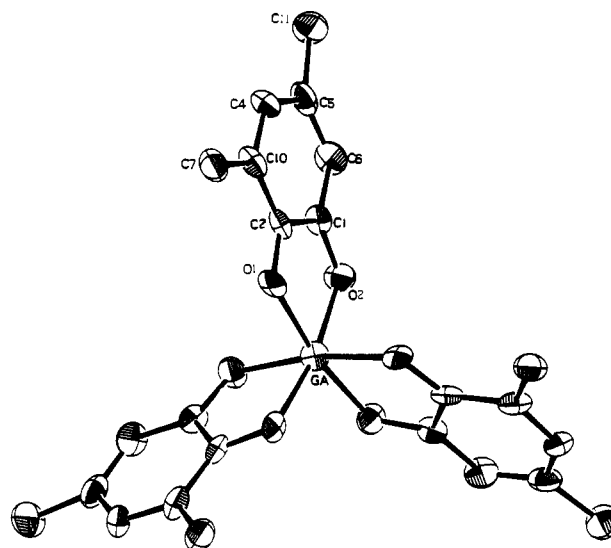
butylcatechol (0.93 g, 4.2 mmol) was treated with sodium hydride (0.10 g, 4.2 mmol) in toluene, giving a blue solution of Na^+TBSQ^- after evolution of hydrogen gas. This solution was stirred for 30 min and then added dropwise to a solution of gallium(III) iodide (0.63 g, 1.4 mmol) in the same solvent. After 4 h, during which the blue mixture became dark green, NaI was separated by filtration, dried and weighed (found 0.60 g, calcd 0.63 g). Evaporation of the filtrate gave green crystals of $\text{Ga}(\text{TBSQ}^*)_3$, identified by its infrared spectrum and metal content (found Ga 9.4). Yield: 1.00 g, 97% based on GaI_3 .

Crystallographic Studies. Crystals of $\text{Ga}(\text{TBSQ}^*)_3$ were grown by allowing *n*-hexane to diffuse into a toluene solution. A suitable crystal was mounted on a glass fibre which was sited in Rigaku AFC6S diffractometer, with graphite moderated Mo $K\alpha$ radiation ($\lambda = 0.71069$ Å; $\mu = 6.72$ cm⁻¹). Cell constants and an orientation matrix for data collection, obtained from a least squares refinement using 20 reflections in the range $12.85 < 2\theta < 18.71^\circ$, corresponded to a rhombohedral (hexagonal axes) cell. On the basis of the systematic absences (hkl : $-h + k + l \neq 3n$) and the successful solution and refinement of the structure, the space group was determined to be $R3(h)$ (No. 146). Details of the data intensity collection and structure refinement are given in Table I.

Of the 1412 reflections which were collected, 1280 were unique ($R_{\text{int}} = 0.089$). The intensities of three representative reflections which were measured after every 150 reflections declined by 0.40%, and a linear correction factor was applied to the data to account for this. Certain weak reflections ($I < 100(I)$) were rescanned to ensure good counting statistics. The data were corrected for Lorentz, polarization and absorption effects.

Treatment of the results by direct methods showed that the gallium atom was in a special position, with C_3 point symmetry. The overall structure was then solved by a combination of direct and Patterson methods.⁵ All the non-hydrogen atoms were refined anisotropically, except for C12 in the *t*-Bu group bonded at C5; the site of this atom was refined isotropically since this gave results better than the anisotropic treatment. The final cycle of full-matrix least-squares refinement, minimizing the function $\sum w(|F_o| - |F_c|)^2$, gave values of $R = 0.050$, $R_w = 0.049$. The molecular structure is shown in Figure 1; final coordinates for the non-hydrogen atoms are given in Table II, and important interatomic distances and angles in Table III.

Neutral atom scattering factors were taken from Cromer and Waber.⁶ Anomalous dispersion effects were included in F_c ; the values for $\Delta f'$ and $\Delta f''$ were those of Cromer.⁸ All calculations were performed using the TEXSAN⁹ crystallographic software package of the Molecular Structure Corp.

**Figure 1.** Molecular structure of $\text{Ga}(\text{TBSQ}^*)_3$: ORTEP diagram, with atoms drawn as 30% probability ellipsoids. Hydrogen atoms have been omitted for the sake of clarity.**Table II.** Final Fractional Coordinates and Isotropic Thermal Parameters (Å²) for Non-Hydrogen Atoms of $\text{Ga}(\text{TBSQ}^*)_3$, with Standard Deviations in Parentheses

atom	x	y	z	B_{eq}^a
Ga	0	0	0.3023	4.34(7)
O1	-0.1076(8)	-0.0234(7)	0.2217(8)	3.8(5)
O2	-0.0989(9)	-0.988(8)	0.382(1)	5.1(7)
C1	-0.181(1)	-0.130(1)	0.344(1)	3.8(7)
C2	-0.186(1)	-0.087(1)	0.257(1)	3.6(7)
C3	-0.235(2)	-0.098(1)	0.040(1)	9(1)
C4	-0.351(1)	-0.184(1)	0.263(1)	5.4(8)
C5	-0.348(1)	-0.227(1)	0.351(1)	5.7(9)
C6	-0.262(1)	-0.201(1)	0.387(1)	5.5(8)
C7	-0.282(1)	-0.074(1)	0.121(1)	5.6(8)
C8	-0.232(1)	0.036(1)	0.127(1)	6.9(9)
C9	-0.381(1)	-0.101(2)	0.093(1)	11(1)
C10	-0.277(1)	-0.117(1)	0.214(1)	4.4(7)
C11	-0.442(1)	-0.300(1)	0.397(1)	7(1)
C12	-0.504(2)	-0.372(2)	0.323(2)	14.9(9)
C13	-0.488(2)	-0.256(2)	0.441(3)	22(2)
C14	-0.426(1)	-0.358(2)	0.468(2)	15(2)

$$^a B_{\text{eq}} = 1/3(\sum_i \sum_j U_{ij} a_i^* a_j^* \cdot a_i a_j).$$

Tables of observed and calculated structure factors, anisotropic thermal parameters, fractional coordinates and isotropic thermal parameters for hydrogen atoms, and the unit cell packing diagram, are available as supplementary material.

EPR Spectra. The EPR spectra were recorded on a Varian E-12 instrument whose field sweep was calibrated with an NMR gaussmeter. The klystron frequency was determined from the resonance field of diphenyldipicrylhydrazide. Low temperature spectra (77 K) were taken with use of a liquid nitrogen dewar insert in the cavity. Variable-temperature and high-temperature measurements were made by using standard Varian accessories. Most of the solutions were made using toluene, pyridine or toluene-pyridine mixtures as the solvent. Spectra in the solvents xylene, hexane, DMF, THF, methylene chloride, tetralin and benzene were also recorded for comparative purposes. In most cases, the concentration of the triradical was 10 mg/mL (0.0137 M), but higher concentrations (up to 30 mg/mL) were used in order to record the low-field part of the frozen solution spectra at $g = 6$. Spectra were obtained at lower concentrations, in an attempt to improve resolution and reduce intermolecular interactions, but the only change in the spectra was a reduced signal to noise. Liquid solution spectra were recorded with 5 mW of power and a modulation 0.1 G or less, while a power level of 20 mW and a modulation amplitude of 5 G were used for frozen solution measurements. The K-band spectrum was recorded on a spectrometer built by Professor F. Holuj in the Physics Department, University of Windsor.

Magnetic Susceptibilities. Magnetization and magnetic susceptibility measurements were made using a variable-temperature vibrating-sample

- Calbrese, J. C. PHASE—Patterson Heavy Atom Solution Extractor. Ph.D. Thesis, University of Wisconsin—Madison, 1972. Beurskens, P. T. DIRDIF: Direct Methods for Difference Structures—An automatic procedure for phase extension and refinement of difference structure factors. Technical Report 1984/1; Crystallography Laboratory: Toernooiveld, 6525 Ed Nijmegen, The Netherlands, 1984.
- Cromer, D. T.; Waber, J. T. *International Tables for X-ray Crystallography*; The Kynoch Press: Birmingham, England, 1974; Vol. IV, Table 2.2A.
- Ibers, J. A.; Hamilton, W. C. *Acta Crystallogr.* **1964**, *17*, 781.
- Cromer, D. T. *International Tables for X-ray Crystallography*; The Kynoch Press: Birmingham, England, 1974; Vol. IV, Table 2.3.1.
- TEXSAN—TEXRAY Structure Analysis Package; Molecular Structure Corp.: Woodlands, TX, 1985.

Table III. Interatomic Distances (Å) and Angles (deg) for Ga(TBSQ)₃, with Estimated Standard Deviations in Parentheses

Distances			
Ga-O1	1.96(1)	C4-C10	1.36(2)
Ga-O2	1.96(1)	C5-C6	1.35(2)
O1-C2	1.28(2)	C5-C11	1.54(2)
O2-C1	1.29(2)	C7-C8	1.56(2)
C1-C2	1.43(2)	C7-C9	1.50(2)
C1-C6	1.38(2)	C7-C10	1.51(2)
C2-C10	1.44(2)	C11-C12	1.51(3)
C3-C7	1.54(2)	C11-C13	1.42(3)
C4-C5	1.42(2)	C11-C14	1.48(3)

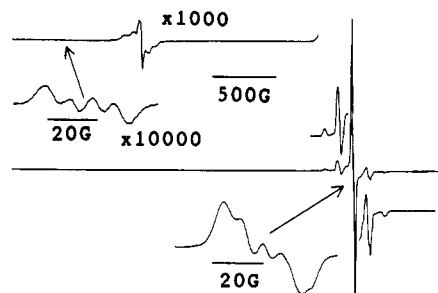
Angles			
O1-Ga-O1'	90.6(5)	C1-C2-C10	119(1)
O1-Ga-O1''	90.6(5)	C5-C4-C10	126(2)
O1-Ga-O2	82.4(4)	C4-C5-C6	117(1)
O1-Ga-O2''	170.1(5)	C4-C5-C11	118(2)
O1'-Ga-O2'	96.4(4)	C6-C5-C11	125(2)
O1'-Ga-O1''	90.6(5)	C1-C6-C5	121(1)
O1-Ga-O2''	96.4(4)	C3-C7-C8	107(1)
O1'-Ga-O2	170.1(5)	C3-C7-C9	110(2)
O1''-Ga-O2'	170.1(5)	C3-C7-C10	110(1)
O1''-Ga-O2	96.4(4)	C8-C7-C9	104(1)
O2-Ga-O2'	91.5(5)	C8-C7-C10	112(1)
O2-Ga-O2''	91.5(5)	C9-C7-C10	113(2)
O2'-Ga-O2''	91.5(5)	C2-C10-C4	115(1)
Ga-O1-C2	112.4(9)	C2-C10-C7	120(1)
Ga-O2-C1	112(1)	C4-C10-C7	125(2)
O2-C1-C2	117(1)	C5-C11-C12	110(2)
O2-C1-C6	122(1)	C5-C11-C13	111(1)
C2-C1-C6	121(2)	C5-C11-C14	110(2)
O1-C2-C1	117(1)	C12-C11-C13	112(2)
O1-C2-C10	124(1)	C12-C11-C14	103(2)
		C13-C11-C14	111(2)

magnetometer system, described previously.¹⁰ Temperatures, measured with a carbon-glass resistance thermometer in close proximity to the sample, are accurate to ± 0.010 – 0.20 K, depending on the range, with a precision substantially better than this. Magnetization and susceptibility data are estimated to be accurate to within 1.5%, also with a precision substantially better yet. Magnetic field values are accurate to 1 G. Susceptibilities have been corrected for demagnetization and for diamagnetism; the latter is estimated to be $\chi_{\text{dia}} = -487 \times 10^{-6}$ emu/mol. The mass of the polycrystalline sample of Ga(TBSQ)₃ used in the measurements was 0.071 75 g.

Results

Preparative Results. The preparation of this compound has been achieved by two complementary routes, and the most important point here is that the reaction between elemental gallium and TBQ leads to a derivative of gallium(III), irrespective of the molar ratio of the reactants. No evidence was obtained for the formation of Ga^I(TBSQ), in sharp contrast to the behaviour of indium in identical conditions.² This result is in keeping with the known trends in the stabilities of the oxidation states of aluminum, gallium, indium and thallium. The compound Ga(TBSQ)₃ is air-stable over months, and soluble in common noncoordinating organic solvents, giving stable solutions, as judged by the absence of any color change or change in the EPR spectrum.

Structure of Ga(TBSQ)₃. The structure of Ga(TBSQ)₃ (Figure 1) confirms the presence of three TBSQ⁻ anions coordinated to a gallium atom which is situated on a 3-fold symmetry axis, so that the ligands are all crystallographically identical. The Ga–O bond length of 1.96(1) Å in the GaO₆ kernel is similar to that (1.952 Å (av)) in Ga(acac)₃ (acac = 2,5-pentanedionate anion).¹¹ The bite angle at gallium is 82.4(4)°, slightly larger than that in In(TBSQ)₃Br₂(pic)₂ (pic = 4-methylpyridine) (74.8(5)°),¹² due presumably to the shortening of the

**Figure 2.** Frozen solution (77 K) EPR spectrum of Ga(TBSQ)₃ in toluene.

M–O bond in Ga–TBSQ⁻ relative to In–TBSQ⁻. The most significant bond distance in the ligand itself is that of 1.28(2) Å (av) for $r(\text{C–O})$; this is typical of semiquinonate species,^{12,13} rather than *o*-quinone or catecholate ligands. The GaO₂C₂ ring is essentially planar (mean deviation 0.011 Å), and the remaining C–C bond distances and angles are all in the normal range. In general, the molecule Ga(TBSQ)₃ is a typical six-coordinate complex of gallium, with an octahedral geometry in the kernel distorted by the demands of the bidentate semiquinonate ligand.

EPR Spectra of Ga(TBSQ)₃ in Noncoordinating Solvents. A solution of Ga(TBSQ)₃ in toluene or other noncoordinating solvents gives a broad unresolved spectrum (line width of about 20 G) at room temperature. At low temperatures the frozen solution spectrum (Figure 2) displays a broad fine structure in the $g = 2$ region, and the strong central line at $g = 2.003$ shows hyperfine splitting due to ⁶⁹Ga ($I = 3/2$, 60.2%) and ⁷¹Ga ($I = 3/2$, 39.8%). The satellite lines at ± 117 G and at ± 233 G from the central line are the “perpendicular” and “parallel” allowed absorptions, respectively. The $\Delta M = 2$ forbidden transitions at half-field are observed with a fine structure and a very weak signal corresponding to the transition $\Delta M = 3$ is observed at $g = 6$. Gallium hyperfine structure is very well resolved in this last transition. The observation of the $\Delta M = 3$ transition and the fine structure in the $\Delta M = 2$ transitions clearly indicate the presence of an $S = 3/2$ spin state. Further analysis of the central peak at $g = 2$, which will be discussed below, reveals that the spectrum also includes the resonance lines from the two $S = 1/2$ states. It will be shown in the theoretical part of the paper that transitions between the quartet ($S = 3/2$) and doublet ($S = 1/2$) states should have detectable intensities. No signals were observed which could be attributed to any transitions between the quartet and doublet states, which suggests that the quartet state is separated from the doublet states by more than 0.3 cm^{-1} owing to the exchange interactions. A K-band spectrum revealed no resonances that could be attributed to quartet–doublet transitions, which suggests that the exchange interaction is much larger than 0.85 cm^{-1} . The sensitivity of the K-band instrument was much poorer than the sensitivity of our X-band spectrometer, however, as no half-field transitions were detected.

Since the spectrum (except for the central absorption) can thus be satisfactorily described as a spectrum of a pure $S = 3/2$ spin state, it was fitted to the spin-Hamiltonian

$$H = \beta_e S \cdot g B + D[S_z^2 - (1/3)S(S+1)] + E[S_x^2 - S_y^2] \quad (1)$$

with an isotropic $g = 2.003$, $D = 108 \times 10^{-4} \text{ cm}^{-1}$, and $E = 0$. An extension of the model of dipolar interactions,¹ which we have applied earlier to the biradicals, predicts a D value of $96 \times 10^{-4} \text{ cm}^{-1}$ for the quartet state, in good agreement with the experimental value. For these calculations the Ga–O distance of 1.96 Å was taken from our X-ray data and the spin densities on the semiquinone rings were assumed to be the same as those used for the biradicals.

(10) DeFotis, G. C.; Failon, B. K.; Wells, F. V.; Wickman, H. H. *Phys. Rev.* **1984**, *B29*, 3795.

(11) Dymock, K.; Palenik, G. J. *Acta Crystallogr., Sect. B* **1974**, *30*, 1364.

(12) Annan, T. A.; Chadha, R. K.; Doan, P.; McConville, D. H.; McGarvey, B. R.; Ozarowski, A.; Tuck, D. G. *Inorg. Chem.* **1990**, *29*, 3936.

(13) Lynch, M. W.; Buchanan, R. M.; Pierpoint, C. G.; Hendrickson, D. N. *Inorg. Chem.* **1981**, *20*, 1038.

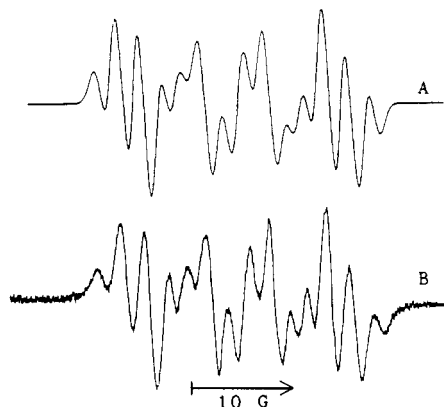


Figure 3. EPR spectra of Ga(TBSQ*)₃ dissolved in pyridine at 90 °C. A is the simulated and B is the experimental spectrum.

The $\Delta M = 2$ transitions at half field contain a sharp signal with gallium hyperfine that cannot be accounted for in our simulations (discussed below), and additional signals were also observed in the $\Delta M = 1$ region for larger concentrations of the triradical. These signals presumably can be ascribed to a small concentration of a biradical of some kind.

The spectra of frozen solutions using other solvents (DMF, THF, methylene chloride, xylene, *n*-pentane, CCl₄, CDCl₃, hexane and tetralin) were similar to that of a toluene solution. Solutions in benzene, paraffin, or heptane showed only one unsplit line at $g = 2$ and a half-field transition at $g = 4$, and this spectrum is almost identical to the powder spectrum at 77 K, due to these solvents failing to form glasses, resulting in aggregation of the solute.

Ga(TBSQ*)₃ in Coordinating Solvents. When dissolved in pure pyridine, Ga(TBSQ*)₃ gives a new resonance whose resolution improves greatly when the solution is heated to 90 °C (Figure 3). The best simulated spectrum (Figure 3) assumes two equivalent hydrogen atoms with $A(^1\text{H}) = 1.84$ G as well as that of the gallium isotopes $A(^{71}\text{Ga}) = 7.40$ G. The frozen solution does not show the spectrum of either a triradical or a biradical, and only one featureless signal at $g = 2.003$ is observed. This $S = 1/2$ species will be referred to as species A. The same spectrum for species A is observed for a solution of the triradical in toluene-pyridine mixtures when the pyridine concentration is much greater than that of Ga(TBSQ*)₃. Intensity measurements show that at 90 °C conversion of Ga(TBSQ*)₃ to A is nearly complete in pyridine. At lower temperatures and for lower concentrations of pyridine in toluene-pyridine mixtures the conversion is less than complete. When these solutions are evaporated to dryness and the residue redissolved in toluene, the spectrum of the triradical reappears. The reaction is apparently endothermic and reversible.

Magnetic Susceptibility. The product of molar susceptibility and Kelvin temperature, $T\chi_M$, of solid Ga(TBSQ*)₃ versus temperature appears in Figure 4. The behavior is unusual in that a clear break is discernible in the 120–140 K range. For $g = 2.0$, $T\chi_M$ should be 0.375 emu K/mol for $S = 1/2$, 1.000 emu K/mol for $S = 1$, 1.876 emu K/mol for $S = 3/2$, and 1.125 emu K/mol for a triradical in which the $S = 3/2$ and $S = 1/2$ states are equally populated. $T\chi_M$ is considerably below the expected value for the triradical but is definitely above the $S = 1/2$ value for most temperatures, although it appears to be approaching that value near 0 K. The break in the region of 120–140 K cannot be attributed to instrumental problems and could indicate a phase transition in this interval.

Since the solution EPR data show the existence of the triradical, at least at the lower temperatures, it was necessary to ascertain if the low susceptibility in the solid is strictly a solid state effect of some sort. We have measured the susceptibility of Ga(TBSQ*)₃

solutions by the Evans method.^{14,15} The results give $\chi_M = 2.56 \times 10^{-3}$ emu K/mol at 296 K, which is essentially the same value as that found in the solid state, so that the low susceptibility is a property of the molecular system rather than a cooperative phenomenon of the crystalline state.

Theory of Spin-Spin Interaction in a Triradical

In an earlier study on biradicals,¹ we were able to treat the spin-spin interactions between the two semiquinone radicals in a quantitative fashion using a point dipole model which assumes that the spin is distributed amongst the eight p_z orbitals of the six carbon and two oxygen atoms. The p orbital was approximated by dividing the spin density, ρ_i , for the atom i into two centers, 0.7 Å above and below the ring.^{16–18} The point dipole interaction was then summed over the 16 centers on each radical ion. A similar approach is used here for the triradical.

The general spin-spin operator has the form¹⁹

$$\hat{H}_{ss} = 4\beta^2 \sum_{j>k} \sum_k [s_j \cdot s_k - 3(s_j \cdot r_{jk})(s_k \cdot r_{jk})/r_{jk}^3] \quad (2)$$

where s_j and s_k are spin operators in units of $\hbar/2\pi$ for electrons j and k and r_{jk} is the distance vector between the two electrons. Using our point dipole model to evaluate the spacial integrals reduces this to a spin-only operator of the form

$$\hat{H}_{ss} = \hat{A} + \hat{B} + \hat{C} + \hat{D} + \hat{E} + \hat{F}$$

$$\hat{A} = A[s_{z1}s_{z2} + s_{z1}s_{z3} + s_{z2}s_{z3}]$$

$$\hat{B} = -(A/4)[(s_1^+s_2^- + s_1^-s_2^+) + (s_1^+s_3^- + s_1^-s_3^+) + (s_2^+s_3^- + s_2^-s_3^+)]$$

$$\hat{C} = C[(s_{z1}s_2^+ + s_1^+s_{z2}) + \epsilon(s_{z1}s_3^+ + s_1^+s_{z3}) + \epsilon^*(s_{z2}s_3^+ + s_2^+s_{z3})] \quad (3)$$

$$\hat{D} = C^*[(s_{z1}s_2^- + s_1^-s_{z2}) + \epsilon^*(s_{z1}s_3^- + s_1^-s_{z3}) + \epsilon(s_{z2}s_3^- + s_2^-s_{z3})]$$

$$\hat{E} = F[s_1^+s_2^+ + \epsilon^*s_1^+s_3^+ + \epsilon s_2^+s_3^+]$$

$$\hat{F} = F^*[s_1^-s_2^- + \epsilon s_1^-s_3^- + \epsilon^*s_2^-s_3^-]$$

The complex constants ϵ , A , C , and F are defined as

$$\epsilon = \exp(2\pi i/3)$$

$$A = 4\beta^2 \sum_i \sum_m \rho_i \rho_m (1 - 3 \cos^2 \theta_{im}) r_{im}^{-3}$$

$$C = 4\beta^2 \sum_i \sum_m \rho_i \rho_m [-(3/2) \sin \theta_{im} \cos \theta_{im} \exp(i\phi_{im})] r_{im}^{-3}$$

$$F = 4\beta^2 \sum_i \sum_m \rho_i \rho_m [-(3/4) \sin^2 \theta_{im} \exp(2i\phi_{im})] r_{im}^{-3} \quad (4)$$

The C_3 symmetry was used to reduce the point dipole summations to summations over one pair of radicals in the equations for A , C , and F . The polar variables r_{im} , θ_{im} , and ϕ_{im} are for the vectors

(14) Evans, D. F. *J. Chem. Soc.* **1959**, 2005.

(15) Ostfeld, D.; Cohen, I. A. *J. Chem. Educ.* **1972**, *49*, 829.

(16) Mukai, K.; Sogabe, A. *J. Chem. Phys.* **1980**, *72*, 598.

(17) Higuchi, J. *J. Chem. Phys.* **1963**, *38*, 1237.

(18) Pullman, A.; Kochanski, E. *Int. J. Quantum Chem.* **1967**, *1*, 251.

(19) McGarvey, B. R. In *Transition Metal Chemistry*; Carlin, R. L., Ed.; Marcel Dekker: New York, 1966; Vol. 3, p 90.

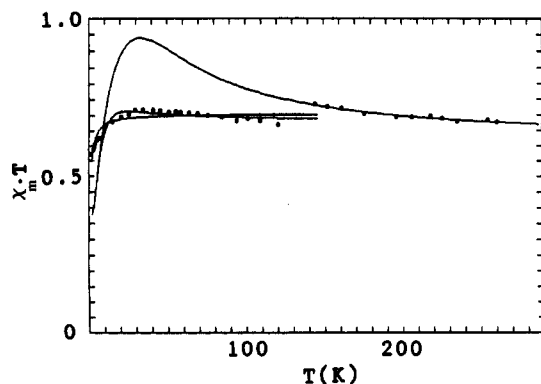


Figure 4. Plot of $T\chi_M$ versus T for solid $\text{Ga}(\text{TBSQ}^*)_3$. The solid curve is a fit of eq 9 to the experimental data. In the region 0–120 K two fits are shown: (1) for all the data and (2) for only the data above 10 K.

connecting the 16 points of spin in each of two semiquinones. The z axis is the C_3 axis of the complex.

Repulsive interactions (exchange interactions) operating through the metal ion can lead to a difference in energy between the quartet state 4A and doublet states 2E . This exchange interaction can be written as

$$\hat{H}_{\text{ex}} = -J(s_1 \cdot s_2 + s_1 \cdot s_3 + s_2 \cdot s_3) \quad (5)$$

The energy difference between the doublet and quartet state due to exchange is then

$$E(^2E) - E(^4A) = 3J/2 \quad (6)$$

Using the above form for \hat{H}_{ss} , \hat{H}_{ex} and well-known quartet and doublet spin functions, the allowed energy states, including the Zeeman interaction, are obtained from the determinant given in Chart I, where $Z_1 = g\beta B_0 \cos \theta$ and $Z_2 = g\beta B_0 \sin \theta \exp(i\phi)$.

The most significant feature of the above determinant is the off diagonal elements that connect the quartet spin states with the doublet spin states. The spin states will be mixed when $3J/2$ is of the same order of magnitude as $|C|$, $|F|$ and transitions will be allowed between the quartet and doublet states unless $3J/2 \gg |C|$, $|F|$. For large $3J/2$ the quartet state can be represented by the spin-Hamiltonian

$$\hat{H} = \beta B \cdot g \cdot S + D[S_z^2 - (1/3)S(S+1)] \quad (7)$$

with $D = 3A/4$. Thus, the nature of the observed EPR spectra will be dependent on the relative magnitude of $3J/2$ vs the spin-spin interaction terms. This is much different from the biradical case where the singlet and triplet states are not mixed by the spin-spin interaction.

Theory of Solution Hyperfine Interaction in Biradicals and Triradicals

In our earlier studies¹ of $\text{M}(\text{TBSQ}^*)_2$ biradicals in solution, the EPR spectrum was a simple doublet with a 3.3-G splitting similar to that observed for the TBSQ^* free radical^{2,20–24} interacting with a metal ion in solution. The splitting is due to the proton bonded to C4, since the spin density at C6 is too small to produce a resolvable splitting for the proton at that site. The appearance of an $S = 1/2$ spectrum for the biradical system that must, in frozen solution, be treated as an $S = 1$ species would appear to suggest that there is no exchange interaction between the two TBSQ^* electrons in these biradicals, which means that the energy separation, J , between the singlet and triplet state of these

biradicals is zero. The theory for the hyperfine interaction of a biradical as a function of the exchange parameter J has been reported by Glarum and Marshall²⁵ for the ^{14}N hyperfine in nitroxide biradicals.

Examination of this theory shows that the expected spectrum for $J = 0$ would be a doublet with a splitting equal to A , which is the same spectrum obtained from a single $S = 1/2$ free radical. When $J \gg A$ the spectrum becomes a 1:2:1 triplet with a splitting of $A/2$. Thus, the value of J in the $\text{M}(\text{TBSQ}^*)_2$ biradicals reported¹ upon earlier must be considerably less than A , which is only 3.3 G or $3.0 \times 10^{-4} \text{ cm}^{-1}$.

In our search of the literature, we have found no similar theoretical consideration of the effect of J on the hyperfine interaction in triradicals. We have done the necessary theoretical calculations and the details are included in the supplementary material. For $J = 0$ the predicted spectrum is the same as that which we found for the biradicals, a doublet with splitting of A . When J is not zero, the exact spectrum depends on the magnitude of J relative to the thermal energy kT , since both the quartet and doublet states are EPR active. We have assumed it likely that $J \ll kT$ and that we would have observed EPR from both states. Our results on the EPR of $\text{Ga}(\text{TBSQ}^*)_3$ support this assumption as will be seen below. The predicted line spectrum for three cases is shown in Figure 5. The most surprising result is for $J \gg A$, in which the quartet state displays a 1:3:3:1 quartet spectrum and the doublet states give a four-line spectrum in which the lines are not equally spaced. The sum of the two spectra give a 1:5:10:10:5:1 sextet with a splitting of $A/3$. This is contrary to what one would have intuitively predicted and such a spectrum, if observed, might lead the unwary to assume that they were observing the free radical EPR of a species with five equivalent proton spins rather than a three-proton system.

Discussion

EPR Spectra of Frozen Solutions of $\text{Ga}(\text{TBSQ}^*)_3$ in Noncoordinating Solvents. The existence of the $\Delta M_S = 3$ resonance in the $g = 6$ region of the spectrum is sufficient evidence that the spectrum contains resonances from the $S = 3/2$ state of the triradical. This conclusion is further supported by special features (discussed below) in the $g = 4$ region of the spectrum and in the center peak of the main resonance centered in the $g = 2$ region of the spectrum. Any resonances from the two $S = 1/2$ states of the triradical would appear in the same region of the spectrum where the center peak of the $S = 3/2$ resonance occurs. We have integrated the spectrum and attempted to compare the intensity of the center peak to the broad $\pm 1/2 \leftrightarrow \pm 3/2$ transitions. The ratio of areas should be 0.67 for just an $S = 3/2$ quartet and two doublet states. Our measurements give a ratio much closer to 0.5 than to 0.67. A more reliable method would be by simulation. We show below by simulation that there is a resonance from $S = 1/2$ states in addition to the $S = 3/2$ resonances.

We have simulated the frozen solution spectrum of our triradical by solving the full matrix of Chart I for $J = 0, 0.10$, and 10 cm^{-1} . The parameters A , C , and F were determined from eq 4 using the X-ray results and spin density parameters ρ_i as determined in our earlier work on biradicals.¹ Taking the y axis to be in the plane of one ligand ring, the calculated values are $A = 128.5 \times 10^{-4} \text{ cm}^{-1}$, $C = (17.0 + 1.2i) \times 10^{-4} \text{ cm}^{-1}$, and $F = (-113.3 + 5.5i) \times 10^{-4} \text{ cm}^{-1}$. The simulated spectra are shown in Figure 6. In this simulation the individual spectra are assumed to be Gaussian with a line width of 6 G. For $J = 0$ the simulated spectrum is very unlike the spectrum observed experimentally (see Figure 2), due to the large coupling terms between the quartet and doublet states which, for small J , completely mixes the states. For $J = 0.10 \text{ cm}^{-1}$, the spectrum begins to resemble the experimental

- (20) Annan, T. A.; McGarvey, B. R.; Ozarowski, A.; Tuck, D. G. *J. Chem. Soc., Dalton Trans.* **1989**, 439.
 (21) Annan, T. A.; Chadha, R. K.; Doan, P.; McConville, D. H.; McGarvey, B. R.; Ozarowski, A.; Tuck, D. G. *Inorg. Chem.* **1990**, *29*, 3936.
 (22) Eaton, D. R. *Inorg. Chem.* **1964**, *3*, 1268.
 (23) Lucken, E. A. C. *J. Chem. Soc.* **1964**, 4234.
 (24) Felix, C. C.; Sealy, R. C. *J. Am. Chem. Soc.* **1982**, *104*, 1555.

- (25) Glarum, S. H.; Marshall, J. H. *J. Chem. Phys.* **1967**, *47*, 1374.

Chart I

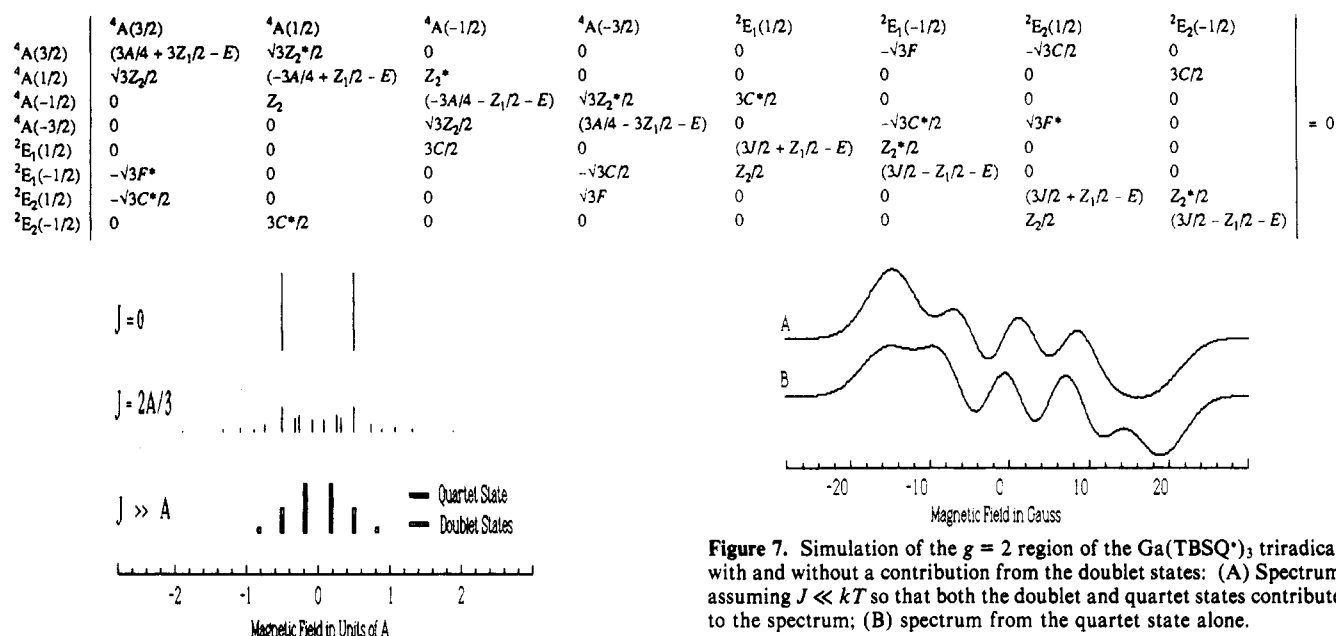


Figure 5. Predicted hyperfine line spectra of a triradical in which each ring has one proton for $J = 0$, $J = 2A/3$, and $J \gg A$. In the last case, it is assumed that $J \ll kT$.

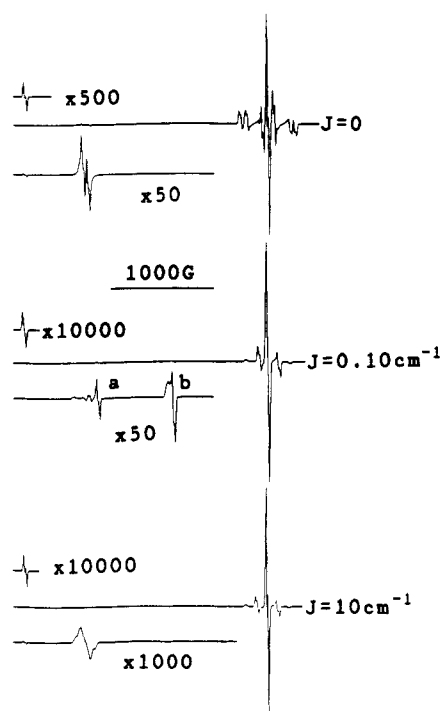


Figure 6. Simulated EPR spectra in the X-band for $\text{Ga}(\text{TBSQ}^\bullet)_3$ for three values of the exchange parameter J . Transitions labeled a and b are transitions between the quartet and doublet states.

spectrum except for the lines labeled a and b in Figure 6, which are transitions between the quartet and doublet states. For $J = 10 \text{ cm}^{-1}$ we have the case where the energy separation between the quartet and doublet states is much larger than both the spin-spin terms and the photon energy of the spectrometer and the agreement between the experimental spectrum and the simulation is very good. We therefore infer that $|J|$ must be greater than 0.8 cm^{-1} , since no quartet-doublet transitions could be detected even in the K-band spectrometer.

Close examination of the simulated spectrum for the $\Delta M = 2$ transition in the $g = 4$ region reveals that this transition in the $S = 3/2$ state must be asymmetrical and broad and that the sharp

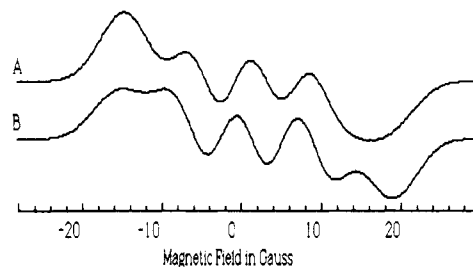


Figure 7. Simulation of the $g = 2$ region of the $\text{Ga}(\text{TBSQ}^\bullet)_3$ triradical with and without a contribution from the doublet states: (A) Spectrum assuming $J \ll kT$ so that both the doublet and quartet states contribute to the spectrum; (B) spectrum from the quartet state alone.

center line with Ga hyperfine splitting observed in the experimental spectrum cannot be a part of the triradical system. The only reasonable explanation of the center peak is the existence of a small concentration of a biradical species which will give a sharp $\Delta M = 2$ transition. Spectra of solutions with a high concentration of the triradical show weak additional peaks in the main portion of the spectrum which could be attributed to this biradical.

The $(M_S = -1/2) \leftrightarrow (M_S = +1/2)$ transition in the quartet state is independent of orientation in first order perturbation theory, but second order terms produce an anisotropy and broadening in this transition for the powder spectrum. The corresponding transitions in the two doublet states should still be isotropic in the powder spectrum. Figure 7 gives a simulation of this portion of the spectrum for the $S = 3/2$ portion of the spectrum only, and for the combined $S = 3/2$ and $S = 1/2$ states, assuming equal population of both the states. Comparison with the experimental spectrum shows that we must be observing the EPR spectrum of both an $S = 3/2$ state and $S = 1/2$ states. This suggests that $|J| < 20 \text{ cm}^{-1}$, since otherwise we could not have nearly equal thermal populations of all the states at liquid N_2 temperatures.

EPR of Solutions of $\text{Ga}(\text{TBSQ}^\bullet)_3$ in Coordinating Solvents. The spectrum of species A obtained by reaction with pyridine displayed a hyperfine splitting for two equivalent protons with the splitting being about half that of the free semiquinone. The most obvious explanation of this spectrum is to assume that species A is $\text{Ga}(\text{TBSQ}^\bullet)(\text{TBC})(\text{py})_2$ in which the two-proton hyperfine spectrum is the result of rapid exchange of the unpaired electron between the two ligand rings giving only half the splitting that comes from the electron residing on only one ring. The reaction occurs first with internal electron transfer to form $\text{Ga}(\text{TBSQ}^\bullet)(\text{TBC})(\text{TQ})$ and the subsequent replacement of the quinone by pyridine. The reaction is reversible as the original triradical is re-formed when the pyridine is evaporated. Similar processes have been observed in related systems.

Magnetic Susceptibility of $\text{Ga}(\text{TBSQ}^\bullet)_3$. Attempts were made to fit the susceptibility data to the model used in the discussion of the EPR data, i.e., a quartet state and two doublet states separated in energy by $3J/2$. In this case the susceptibility χ_M is given by

$$\chi_M(T) = (0.375 \text{ emu K/mol})/T[5.0 + \exp(-\delta_1/kT)]/[1 + \exp(-\delta_1/kT)] \quad (8)$$

where δ_1 is the energy separation between the doublet and quartet states ($3J/2$). In eq 8 it was assumed that $g = 2.0$ for both states,

as this is the value determined from our EPR results. It is not possible to fit this equation to the data, however, as δ_1 would have to be -247 cm^{-1} to obtain the room temperature value of χ and no reasonable fit can be obtained over the temperature range measured. The experimental susceptibility is just too small to be accounted for by the triradical model.

It is apparent from Figure 4 that at high temperatures the percentage of $S = 1/2$ states is much higher than our triradical model predicts and that the lowest state of the molecule is $S = 1/2$ when $T \rightarrow 0\text{ K}$. Since there is no evidence of antiferromagnetic coupling the only model that could account for all our experimental results is one that assumes there is an additional set of doublet states that becomes populated at higher temperatures. This is not an unreasonable assumption, since the reaction of $\text{Ga}(\text{TBSQ}^*)_3$ with pyridine in solution reveals that there is a thermally accessible $S = 1/2$ form, namely $\text{Ga}(\text{TBSQ}^*)(\text{TBC})(\text{TBQ})$, which is 6-fold degenerate. In this model, we take χ_M to be given by the equation

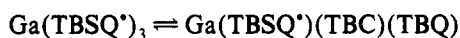
$$\chi_M = \chi(\text{triradical}) p + \chi(S = 1/2)(1 - p) \quad (9)$$

where p = mole fraction of triradical, $\chi(\text{triradical})$ is from eq 8, and $\chi(S = 1/2)$ is $0.375/T$. From thermodynamics we have

$$p = (1 + K)^{-1}; \quad K = A_0 \exp(-\delta_2/kT);$$

$$A_0 = \exp(\Delta S/k) \quad (10)$$

where K is the equilibrium constant for the reaction



and δ_2 and ΔS are the enthalpy and entropy changes for the reaction, respectively. The best fits of eq 9 are plotted as solid lines in Figure 4. The high-temperature data above 140 K can be reasonably fitted with $(\delta_1 + \delta_2) = 70 \pm 1\text{ cm}^{-1}$ and $A_0 = 2.18 \pm 0.05$. In Figure 4, we have plotted eq 9 with $\delta_2 = 78.5\text{ cm}^{-1}$, $A_0 = 2.19$, and $\delta_1 = -9\text{ cm}^{-1}$. The low-temperature data below 120 K could not be fitted as satisfactorily. We show two fittings in Figure 4, one for points above 10 K, in which the best parameters were $\delta_1 = -8.95\text{ cm}^{-1}$, $\delta_2 = 13.85\text{ cm}^{-1}$, and $A_0 = 1.47$, and the second for all points, in which the best parameters were $\delta_1 = -0.60\text{ cm}^{-1}$, $\delta_2 = -0.76\text{ cm}^{-1}$, and $A_0 = 1.33$. Neither of these can be considered a good fit.

One serious problem with the model we are using is the assumption that δ_2 and ΔS are independent of temperature even close to 0 K. The above attempts to fit the low-temperature data showed that the lowest temperature points could only be fitted if both energy parameters were close to zero, but a good fit in the higher temperature region requires that δ_2 must be of the order of $15\text{--}30\text{ cm}^{-1}$. We have found that an excellent fit to all the low-temperature data is possible if we allow a variation in δ_2 with temperature, with $A_0 = 2.1$ and δ_2 varying from near zero at $T = 0\text{ K}$ to about 30 cm^{-1} at 120 K. The fitted values of A_0 are consistent with our model. If ΔS were only determined by the change in degeneracy of the state when going from the triradical to the monoradical, we would expect A_0 to be 1.5 since at higher temperatures the degeneracy of the triradical is 8 and that of the monoradical is $6 \times 2 = 12$. The break in the temperature data in the region 120–140 K could be a phase transition in this temperature range that changes mainly δ_2 .

Close inspection of the susceptibility below 10 K discloses small anomalies near 3.5 K and near 1.95 K. There is, however, no clear indication of a magnetic phase transition in this region. The molar magnetization versus field at a few temperatures is shown in Figure 8. The 12.03 K isotherm is essentially linear up to 15.9 kG while the 4.23 K isotherm shows slight curvature at higher fields. The 1.94 K isotherm displays substantial curvature, and this is most likely due to the thermal energy becoming comparable to the energy separations δ_1 , δ_2 , and the Zeemann energy.

Room-Temperature EPR Spectrum of $\text{Ga}(\text{TBSQ}^*)_3$. The susceptibility results suggest the existence of a monoradical Ga -

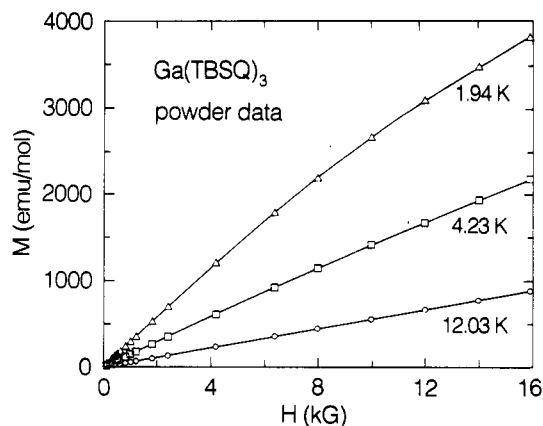


Figure 8. Plot of the molar magnetization versus field at three different temperatures.

$(\text{TBSQ}^*)(\text{TBC})(\text{TBQ})$ which is present in better than 50% concentration at room temperatures. It is difficult to show the existence of this monoradical from the EPR spectra by comparing the intensity of the $-1/2 \leftrightarrow 1/2$ line to those of the $\pm 1/2 \leftrightarrow \pm 3/2$ lines because the ratio changes only from 0.50 to 0.55 when we have a pure triradical to a 50–50 mixture of the triradical states and monoradical states. The problem comes from the fact that the $-1/2 \leftrightarrow 1/2$ transition for an $S = 3/2$ state is 4 times the intensity of a simple $S = 1/2$ state. The presence of both a triradical (which would give a sextet H spectrum with $A/3$ splitting) and the monoradical (which would give a quartet H spectrum with $A/3$ splitting due to the unpaired electron being rapidly exchanged between the three rings) in solution easily accounts for the featureless broad spectrum observed at room temperature for $\text{Ga}(\text{TBSQ}^*)_3$.

Conclusions

We have synthesized and characterized a compound which we formulated as $\text{Ga}(\text{TBSQ}^*)_3$ and have determined its structure through X-ray crystallographic analysis. EPR and magnetic susceptibility studies have shown that this molecule exists in two forms, triradical $\text{Ga}(\text{TBSQ}^*)_3$ and monoradical $\text{Ga}(\text{TBSQ}^*)(\text{TBC})(\text{TBQ})$, with the triradical form being marginally lower in energy. There is no evidence in the X-ray results for unusual C–O bond lengths or for large thermal parameters in the GaO_2C_2 ring. The triradical has both a quartet state and two doublet states with the doublet states being a few cm^{-1} lower in energy than the quartet state. The existence of two thermally accessible forms of $\text{Ga}(\text{TBSQ}^*)_3$ comes as a surprise, and indicates that a more careful study of similar systems⁴ that have been characterized as triradicals should be undertaken. We are initiating such studies in our laboratories.

Acknowledgment. This work was supported in part by Operating Grants (to B.R.M. and D.G.T.) from the Natural Sciences and Engineering Research Council of Canada and by NSF-Solid State Chemistry-Grant No. DMR-8906337 (to G.C.D.) from the National Science Foundation. We thank Professor F. Holuj, Department of Physics, University of Windsor, for recording the K-band spectrum.

Supplementary Material Available: Tables giving anisotropic thermal parameters, hydrogen atom locations, and the least-squares plane of the GaC_2O_2 ring, in addition to a cell diagram and a textual presentation of the theory of solution hyperfine interaction in a triradical (7 pages). Ordering information is given on any current masthead page.